

Learning from SAM: Harnessing a Foundation Model for Sim2Real Adaptation by Regularization

Mayara E. Bonani¹
mayarabonani@uni-bonn.de

Max Schwarz^{1,2,3}
schwarz@ais.uni-bonn.de

Sven Behnke^{1,2,3}
behnke@cs.uni-bonn.de

¹Autonomous Intelligent Systems, Computer Science VI, University of Bonn, Germany

²Lamarr Institute for Machine Learning and Artificial Intelligence, Germany

³Center for Robotics, University of Bonn, Germany

Abstract—Domain adaptation is especially important for robotics applications, where target domain training data is usually scarce and annotations are costly to obtain. We present a method for self-supervised domain adaptation for the scenario where annotated source domain data (e.g. from synthetic generation) is available, but the target domain data is completely unannotated. Our method targets the semantic segmentation task and leverages a segmentation foundation model (Segment Anything Model) to obtain segment information on unannotated data. We take inspiration from recent advances in unsupervised local feature learning and propose an invariance-variance loss over the detected segments for regularizing feature representations in the target domain. Crucially, this loss structure and network architecture can handle overlapping segments and oversegmentation as produced by Segment Anything. We demonstrate the advantage of our method on the challenging YCB-Video and HomebrewedDB datasets and show that it outperforms prior work and, on YCB-Video, even a network trained with real annotations. Additionally, we provide insight through model ablations and show applicability to a custom robotic application.

I. INTRODUCTION

Domain Adaptation is the art of transferring knowledge learned from one domain to another domain, usually the application domain. For roboticists in particular, the very idea of using out-of-domain data is very appealing, since target domain data is usually not available in quantities that are interesting for modern deep learning approaches, and target domain *annotations* are even more costly to obtain.

Synthetic data is one kind of out-of-domain data, which is particularly cheap to generate. It can get close to the target domain in many properties, but still suffers from *domain gap*, the effect that the data distributions do not overlap perfectly and thus a trained model cannot generalize from training domain to application domain. In the case of synthetic data, this is more specifically also called the *Sim2Real gap* [1].

While there is ongoing research on decreasing this gap through improvement of synthetic generators [2], [3] or learning to adapt training data to fit a target distribution [4], we choose to approach the issue from another, orthogonal direction: Can we regularize the model in a task-specific manner so that it performs more robustly in the target domain?

Recently, *foundation models*, i.e. very large models trained on internet-scale datasets, have been released for various tasks. One of these, the Segment Anything Model (SAM) [5] targets segmentation tasks and demonstrates impressive performance

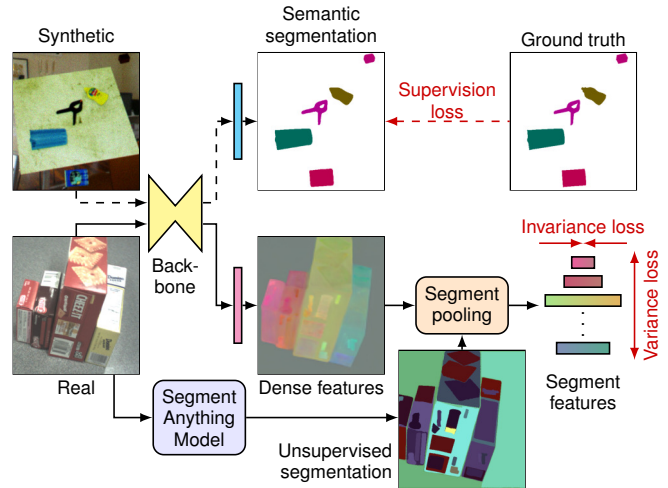


Fig. 1. Hybrid learning from annotated synthetic data (top path, dashed) and unannotated real data (bottom path, solid). For synthetic data, ground truth is available. For real data, projected dense features are aggregated using segment information obtained from Segment Anything Model (SAM). An invariance loss forces feature vectors of the same segment closer together, while a variance loss spreads segment means apart. Both branches of the network train the backbone and thus benefit from each other.

in prompted settings, i.e. where there is some knowledge of the target objects’ location. Still, SAM is not suitable for most robotic applications as-is, since it does not have any knowledge of the target semantics (e.g. object classes) and is much to compute-intensive for real-time application.

In this work, we explore a way of distilling the general “objectness” knowledge learned by SAM to achieve robust domain adaptation of semantic segmentation networks. In particular, we use SAM to generate a regularization signal for the task model—derived from unlabeled target domain data by pooling dense features into detected segments (see Fig. 1). We then use an invariance-variance loss scheme inspired by recent advancements in self-supervised feature learning [6], [7] to regularize the learned features on unannotated real data.

Our method significantly outperforms a prior Sim2Real method [4] and beats even models trained with real labels.

Our contributions include:

- 1) a segment pooling scheme which uses pre-extracted SAM segments to aggregate features,
- 2) a loss formulation that allows self-supervised learning

on a combination of annotated synthetic data and unannotated real data,

- 3) thorough evaluation on the challenging YCB-Video and HomebrewedDB datasets and two different synthetic data generators,
- 4) ablations showing the influence of hyperparameters, and
- 5) quick application to a custom robotic problem setting.

II. RELATED WORK

Unsupervised domain adaptation is a wide and active research field. For a general overview, we refer to Liu *et al.* [8]. We will discuss methods most related to our approach here.

◦ *Synthetic Data.* Annotated data is difficult and costly to obtain, in particular for the large variety of applications in robotics. As an alternative, synthetic data generation is a promising approach, since precisely-labeled training data can be generated cheaply. Denninger *et al.* [3] propose BlenderProc, focused on the realism of generated images, employing offline rendering techniques such as path tracing using the well-known Blender software. Schwarz and Behnke [2] introduce the Stilleben framework, which generates training data for perception tasks such as semantic segmentation, object detection, and pose estimation. The images provided by Stilleben are obtained through physics simulation of object meshes and rasterization, allowing the objects to have a randomized appearance and material parameters in addition to noise and transformations that simulate the camera sensors in a scene. In contrast to BlenderProc, Stilleben can be used online due to its fast GPU-based rendering pipeline. For this work, we use both BlenderProc and Stilleben in order to evaluate our method for different synthetic data generators.

◦ *Unsupervised Learning.* If only unlabeled data is available, one can also turn to unsupervised techniques for learning robust features. Joint embedding architectures represent one of the main streams in recent works. Bardes *et al.* [6] proposed a self-supervised method for training such architectures, called Variance-Invariance-Covariance Regularization (VICReg). First, the variance regularization term is defined as a hinge function on the standard deviation of the embeddings along the batch dimension and above a given threshold. It thus forces the embedding vectors of samples within a batch to be different. Two augmentations of the same sample, in contrast, are forced closer together by the invariance term. Finally, the covariance term encourages decorrelated feature dimensions. Overall, the authors show that their regularization stabilizes training and leads to robust learned features.

The VICReg approach performs well for classification tasks, but it is not suitable for image segmentation because it removes spatial information to satisfy the invariance criterion. To address semantic segmentation tasks, the model needs to focus on learning local information. With this motivation, the VICRegL method by Bardes *et al.* [7] considers global and local features simultaneously. At the global level, the VICReg criterion is applied in the same way as before. At the local level, VICRegL uses spatial information to match feature vectors that are pooled from nearby regions in the

original image (pixels that have a small distance between them) or by small feature distance in the embedding space. The VICReg criterion is applied only to the top- γ l^2 nearest-neighbor (NN) feature vectors considering image locations and feature maps. Our loss formulation is inspired by the VICReg criterion, but in contrast to VICRegL, our method leverages external (over-)segmentation information generated by SAM to derive intra-frame correspondences. Another difference is that we employ a modern segmentation backbone architecture which is able to generate features in a much higher resolution.

Perhaps most related to our approach, Hénaff *et al.* [9] group local feature vectors according to a simple unsupervised pre-segmentation and apply a contrastive objective to each object-level feature separately. Their contrastive objective maximizes the similarity across views of local features, which represent the same object, while minimizing similarity for local features from different objects. In contrast to their work, which focuses on self-supervised pretraining, our method makes use of the available supervision on synthetic data during training.

◦ *Domain Adaptation.* Although synthetic data is a viable solution to the annotation bottleneck problem, it suffers from the domain gap between synthetic and real data, i.e. the discrepancy between the statistical properties obtained by the synthetic data distribution and the real data distribution. To overcome the performance degradation when the model is trained using real images, Imbusch *et al.* [4] suggested a multi-step learning-based approach to perform synthetic-to-real domain adaptation and consequently minimize the domain gap. Similar to our work, synthetic images are generated using Stilleben [2]. The images are then fed into a domain adaptation network, which outputs images more similar to the real dataset while preserving annotations. This domain adaptation approach is based on Contrastive Unpaired Translation (CUT) [10], which is an image-to-image translation technique aimed at preserving the image content while adapting the appearance to a target domain. CUT is a GAN-based approach that uses a contrastive loss on image patches to achieve content preservation by ensuring that a patch of the translated image has more information in common with the same patch in the source image than with other patches from the source image. Instead of applying CUT to images at full resolution, Imbusch *et al.* [4] used a patch-based application of the CUT approach and improved the segmentation results obtained from synthetic data for two robotics datasets. Finally, the adapted images are used for training the task network. In contrast to this method, we do not adapt training images, but instead perform the adaptation while training the task network by regularizing its performance on unannotated data.

◦ *Segment Anything Model (SAM).* Foundation models (such as BERT [11], RoBERTa [12], and GPT-4 [13]) enable powerful generalization for tasks and data distributions beyond those seen during training. Kirillov *et al.* [5] focused on building a foundation model for image segmentation. The promptable segmentation task is to return a valid segmentation mask given any segmentation prompt, such as a set of foreground and background points or a rough bounding box specifying

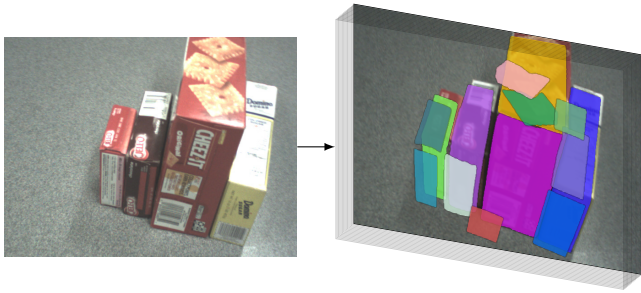


Fig. 2. Segments predicted by SAM in its “segment everything” mode, shown stacked in 3D on top of the reference image. Note how the segments overlap and over-segment the image. We only show a small number of segments for clarity.

what to segment in an image. The Segment Anything Model (SAM) can adapt to diverse segmentation tasks. Importantly for a foundation model, the authors collected the Segment Anything Dataset, SA-1B, which consists of 11 million diverse, high-resolution, licensed, and privacy protecting images and 1.1 billion high-quality segmentation masks. The dataset was collected through model-in-the-loop dataset annotation, leveraging weaker versions of SAM to annotate more training data for later stronger versions.

Although the model has some limitations, such as missing fine structures, segmenting small disconnected components, etc., the trained SAM model can segment unfamiliar objects and images without requiring any training or annotations and can be used for different tasks, as long as a prompt is available. Additionally, it was designed to be able to naturally handle ambiguity, such as a prompt meaning smaller (e.g. shirt) or bigger (e.g. person) scene entities. Therefore, its output predicts multiple masks for a single prompt, resulting in segments that intersect each other. SAM cannot be applied directly for usual semantic segmentation tasks, though, because it has no knowledge of the target classes, making additional processing necessary to obtain only one label per pixel.

In parallel with our work, Kim *et al.* [14] proposed a method for utilizing SAM for hierarchical decomposition of scenes. A very similar contrastive loss structure is used to ensure parts that are grouped by SAM end up with similar features. Notably, the authors introduce a multi-scale architecture to extend the range of the built grouping hierarchy. The method is applied to 3D neural radiance fields, focusing on high-fidelity offline decomposition of pre-recorded 3D scenes. In contrast, our method is applied as regularization during training of a task network, which is later capable of real-time operation on novel scenes, and, through synthetic supervision, produces semantics.

III. METHOD

We will now describe our method in detail. Fig. 1 shows the general information flow and Fig. 3 zooms into the trained network.

A. SAM Preprocessing

The Segment Anything Model (SAM, [5]) allows zero-shot segmentation given a point, mask, or even textual prompt. It

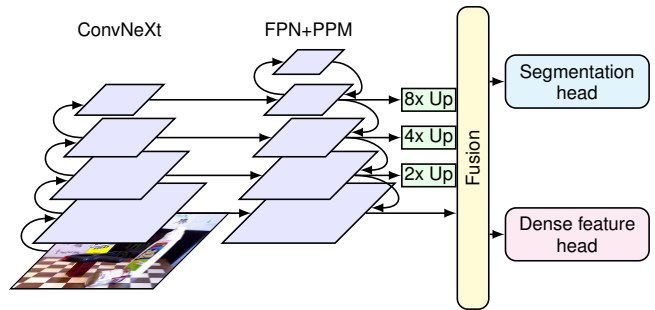


Fig. 3. Detailed architecture of the backbone with the segmentation head and the dense feature head. “Up” denotes a bilinear upsampling layer.

has learned a general objectness concept which allows it to predict the most likely segment belonging to a prompt. We use the default “automatic” mask prediction mode of SAM, which queries the model with a grid of query points to segment “everything” in the image. The default settings are chosen for SAM with a ViT-H backbone. The number of points to be sampled along each side of the image is 24.

Because the SAM results only depend on the input image, SAM segmentation can be done in a preprocessing step. This is most welcome, since SAM execution is compute-intensive.

Because each segment is predicted in isolation, SAM produces an oversegmentation of the image with overlapping masks (see Fig. 2). To deal with this effect, we do not directly use the SAM segments to e.g. generate some pixel-wise pseudo labels, which would be difficult due to the overlapping (see Section IV-E for an experiment showing this). Instead, our proposed loss formulation is able to deal with this ambiguity (see Sec. III-E).

B. Modern Segmentation Backbone

The backbone of our network follows a standard architecture in recent segmentation works [15]–[17]: We combine a strong ConvNeXt-L [17] pretrained on ImageNet classification with a Feature Pyramid Network (FPN) [18], which propagates highly semantic features from higher, low-resolution layers back to the lower, high-resolution layers (see Fig. 3). Inspired by Xiao *et al.* [15], we also add an additional Pyramid Pooling Module (PPM) [19] on top of the feature pyramid, which improves global context by even further spatially aggregating features. A single fusion layer then produces a single feature map with 512 channels and high resolution. The resulting structure is similar to the one evaluated in [17] for segmentation tasks. Congruent with ConvNeXt, all our network layers use GELU activations.

C. Segmentation Head

A single convolutional layer with kernel size 1×1 computes the semantic segmentation result (i.e. class logits). On synthetic images, where annotations are available, this layer and the backbone are trained using the standard cross entropy loss

$$\mathcal{L}_{\text{Sup}} = \frac{1}{|I|} \sum_{p \in I} -\log \frac{\exp(x_{p,y_p})}{\sum_{c=1}^C \exp(x_{p,c})}, \quad (1)$$

where $p \in I$ are the pixels of the current frame, $x_{p,c}$ is the logit prediction on pixel p for class $c \in C$, and y_p is the ground truth class for pixel p .

For images without annotations, this output provides a compatible semantic segmentation but due to the lack of ground truth, it cannot be used for training.

D. Dense Feature Head

Inspired by VICReg [6] and VICRegL [7], we add a projection block for the self-supervised feature learning on real images. This projection block consists of two layers that bring the feature dimension first down to 256 and then to D . In our experiments we choose $D = 3$, which has the advantage of being easily visualizable as RGB colors. Low dimensionality in contrastively learned features is a common choice [20] and indeed, we did not observe higher performance in experiments with higher D (see Section IV-E).

The fact that the self-supervised feature learning uses a different projector than the semantic segmentation provides the necessary decoupling: Since SAM oversegments the image, it is important that the segmentation head can ignore some fine-grained differences visible in the dense feature output (see the exemplary SAM output in Fig. 2).

E. Segment Pooling

Our way to use the SAM annotations is to pool together features that belong to the same segments as detected by SAM. Hénaff *et al.* [9], for instance, jointly pool the feature vectors coming from the same region in the mask and contrast the resulting vectors between each other with a contrastive loss function. This allows feature vectors spatially far away in the original image to be pooled together if they belong to the same object. Following the same idea, we use the SAM segments to pool together regions in the feature maps. We highlight that we do not make use of any label, but instead use SAM segments to regularize the predicted dense features, instilling a sense of objectness into our backbone and the dense feature head—as guided by SAM.

After upsampling the output of the dense feature head to the image resolution, our pooling block computes the mean $\mu_i \in \mathbb{R}^D$ and the unnormalized variance vector $v_i \in \mathbb{R}^D$ for each segment $i \in \{0, \dots, N\}$:

$$\mu_i = \frac{1}{|S_i|} \sum_{p \in S_i} z_p, \text{ and} \quad (2)$$

$$v_i = \sum_{p \in S_i} (z_p - \mu_i)^{\odot 2}, \quad (3)$$

where S_i is the set of pixels belonging to segment i , z_p is the feature vector located at p , and $(\cdot)^{\odot 2}$ denotes the element-wise squaring operation (Hadamard power). The variance is not normalized by pixel count, since this would give equal importance to segments of any size, resulting in an undesired focus on smaller segments. Instead, we give each pixel of each segment equal weighting (see below).

◦ *Invariance Loss.* The first information we can obtain from SAM is that pixels from the same segment are likely to belong

to the same object. Thus, we strive to keep segment variance low. Therefore, we define the invariance loss

$$\mathcal{L}_{\text{Inv}} = \frac{\frac{1}{D} \sum_{i=1}^N \|v_i\|_1}{\sum_{i=1}^N |S_i|}. \quad (4)$$

◦ *Variance Loss.* The second insight is that two different SAM segments are likely from different objects. We thus expect a minimum margin β between means, leading to the variance loss

$$\mathcal{L}_{\text{Var}} = \frac{2}{N(N-1)} \sum_{i \neq j} \max(0, \beta - \|\mu_i - \mu_j\|_2), \quad (5)$$

where we choose $\beta = 0.5$ as in [6].

We note that the assumption behind Eq. (5) does not hold in two cases: 1) Overlapping segments. In that case, variance and invariance loss will both be applied to the same pixels. This balanced regularization yields similar, but distinct features for objects and their parts, as discussed in Section IV-D and shown in Fig. 5, and thus poses no problem. 2) Segments that do not intersect, but belong to the same object. In that case, SAM gave us no indication that the two segments belong to each other and we have to assume they are separate. We note that the segmentation head learns to produce the same class label for non-overlapping segments through the synthetic supervision.

We emphasize that our primary goal is not to learn dense features with particular properties, but to regularize the segmentation network. The segmentation head can, by learning from its synthetic supervision, decide to ignore or accept features that arise from SAM regularization, as long as these under- and oversegmentation effects also occur in synthetic data. We also note that it would be possible to further refine or filter SAM masks by using the model trained on synthetic data as a teacher. However, our regularization approach is designed to help especially in the cases where the unregularized method would make segmentation mistakes, and we argue that it does not help to commit to these mistakes by focusing on SAM masks that under- or oversegment the target object. Indeed, Section IV-E shows that “intelligently” generating pseudolabels in such a manner does not improve performance.

Bardes *et al.* [6] also propose a covariance loss which helps to keep individual feature dimensions decorrelated. In our experiments, we found that this component is unnecessary in our case, most likely because of the presence of supervision on synthetic images, which yields backbone outputs (before the heads) that correspond to object classes.

The total loss in the self-supervised case on real images is thus

$$\mathcal{L}_{\text{real}} = \alpha (\mathcal{L}_{\text{Inv}} + \mathcal{L}_{\text{Var}}), \quad (6)$$

where $\alpha = 0.05$ is used to scale the loss in relation to the supervised loss on synthetic images, bringing them approximately to the same magnitude on the YCB-Video dataset.

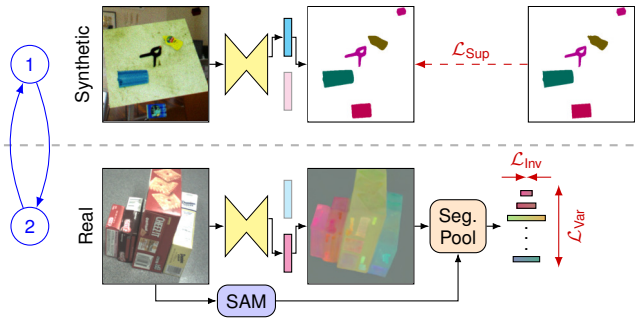


Fig. 4. Alternating training of the backbone and heads on synthetic (top) and real (bottom) data.

IV. EVALUATION

A. Training Details

We follow the training and evaluation protocol of Imbusch *et al.* [4]: Training is conducted over 300 epochs of 1500 frames each with a batch size of 1. Synthetic data is either generated on the fly (so that a frame is never repeated) or selected randomly from available frames. Accordingly, for real data the 1500 frames are randomly chosen from the entire dataset for each epoch. Similar to [4], an exponential moving average (EMA) version of the model is used for evaluation. We report the mean intersection over union (mIoU) score on the test dataset, averaged over the last 50 training epochs, which eliminates any remaining short-term training effects (see [4] for details).

Our full model requires both synthetic and real images. To keep RAM usage low, we follow an alternating training scheme (see Fig. 4), where in each iteration first a synthetic image is processed and then a real image. The supervised and self-supervised losses are thus only added stochastically over the course of optimization. Training was conducted on NVIDIA RTX A6000 and A100 GPUs.

B. Datasets

As in [4], we evaluate our method on the YCB-Video [21] and HomebrewedDB [22] datasets. Both datasets are part of the well-known BOP challenge [23] and contain object meshes—a prerequisite for generating synthetic data.

- *YCB-Video* contains 21 YCB [24] objects captured with an RGB-D camera in 92 videos, totaling approx. 134k frames. The frames exhibit difficult lighting conditions and camera noise. For synthetic data, we use Stilleben [2], which generates physically plausible arrangements and renderings on the fly during training.

- *HomebrewedDB* is a slightly smaller dataset with 13 different scenes. Following [4], we only use the PrimeSense frames. The “val” split is used for training, and the “test” split for evaluation (HomebrewedDB does not contain a “train” split with real data). The semantic segmentation is trained and evaluated only on the BOP test objects. For synthetic data, we use the BlenderProc4BOP synthetic frames provided by BOP. Imbusch *et al.* [4] used Stilleben data for HomebrewedDB, but since Stilleben is not well adapted to HomebrewedDB, which

TABLE I
SEMANTIC SEGMENTATION RESULTS

Method \ Dataset	Mean IoU	
	YCB-Video [21]	HomebrewedDB [22]
Imbusch <i>et al.</i> [4]		
- real labels	0.770	0.737
- synthetic only	0.701	0.481 ¹
- full	0.763	0.558 ¹
Ours		
- real labels	0.839	0.883
- synthetic only	0.807	0.748
- CUT [4] only ²	0.814	-
- full	0.853	0.787 ³

Note: “real labels” is a baseline which has access to real supervision.

¹ [4] uses Stilleben [2] synthetic data, we use BlenderProc4BOP for HomebrewedDB.

² Training our backbone on CUT-refined synthetic data.

³ Model was trained for only 200 epochs.

contains many occluding background objects, we observed lower performance. The BlenderProc4BOP images also allow us to demonstrate our method on a second type of synthetic data.

C. IoU Metric

To stay comparable with prior work [2], [4], we evaluate our models using the mean intersection over union metric, which is defined as follows:

$$\text{IoU}_c(I) = \frac{|P_c(I) \cap G_c(I)|}{|P_c(I) \cup G_c(I)|}, \quad (7)$$

$$\text{mIoU} = \frac{1}{|\mathbf{I}|} \sum_{I \in \mathbf{I}} \frac{1}{|C_I|} \sum_{c \in C_I} \text{IoU}_c(I), \quad (8)$$

where $P_c(I)$ are the pixels predicted for class c on image I , $G_c(I)$ is the corresponding ground truth, C_I are the classes present in frame I , and \mathbf{I} is the set of test images.

D. Results

Table I reports semantic segmentation results on YCB-Video and HomebrewedDB. We compare our results with those of Imbusch *et al.* [4], since they address the same problem setting. Similar to their evaluation, is not our intention to beat the overall state-of-the-art in semantic segmentation, but instead show the improvement gained by using our method when applied to a straightforward segmentation model.

As a first observation, our more modern segmentation backbone based on ConvNeXt and FPN+PPM compared to the older RefineNet [25] used in [4] is able to achieve much higher mIoU on the baseline of real annotated data for both datasets. To analyze the impact of this further, we train an ablation of our backbone with CUT-refined data, like in [4]. This combination achieves similar results as compared to training our backbone directly on synthetic data. In conclusion, the more modern backbone architecture already provides the robustness that was induced through data augmentation in [4].

Furthermore, our method not only outperforms a network purely trained on synthetic data, but also beats the real baseline on YCB-Video. On HomebrewedDB, our method provides a

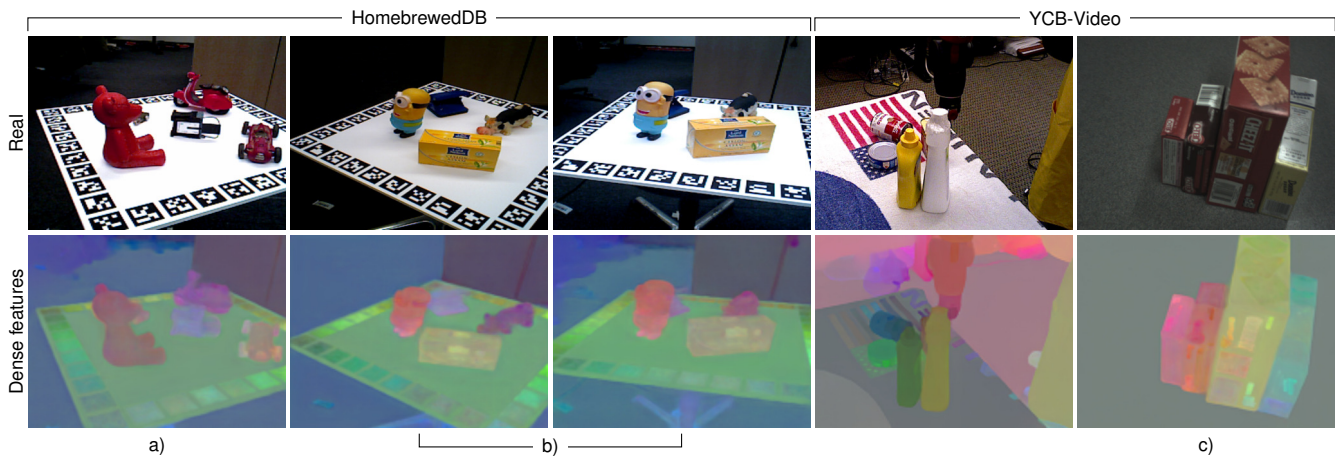


Fig. 5. Learned dense features normalized and visualized as RGB colors. The upper row shows input images from HomebrewedDB (left) and YCB-Video (right). The bottom row shows features learned by the network in self-supervised fashion. Note that a) features correspond well to objects, b) features are stable under camera motion, and c) SAM oversegmentation leads to object parts such as text receiving slightly different but related locations in feature space.

decent advantage over synthetic data alone, but does not reach the performance possible from real annotations. This may be due to the smaller quantity and especially the smaller diversity of available real data.

Figure 5 shows the learned dense features qualitatively. It is immediately evident that the learned features correspond well to the objects to be segmented and it can be concluded that learning such a representation is highly likely to be helpful for the semantic segmentation task. The fact that the learned representations remain stable under camera motion is a further indicator that the network is learning a shared representation for semantic segmentation and dense features—since the invariance-variance loss alone does not demand such coherence. Interestingly, the feature visualizations exhibit the over-segmentation done by SAM. Small parts of objects, such as text and/or markings receive slightly different feature values in order to satisfy the variance loss. Still, through the decoupled two-head design, this does not impact segmentation performance.

If we analyze the regularizing effect of SAM on the segmentation output, we can see that using the full pipeline encourages more complete segments (see Figs. 6 and 7). In contrast, a model trained only on synthetic data will often only detect parts of objects. In our opinion, this means that the general sense of “objectness” learned by SAM has been successfully distilled and combined with the target domain semantics by our approach.

Executing our model requires only one forward pass and is possible in real-time on an NVIDIA RTX A6000 GPU (40 ms per 640×480 frame). In contrast, the SAM backbone with grid prompting takes more than one second to process the same frame.

E. Additional Ablations

We performed additional ablations to investigate the contribution and parameters of SAM regularization.

a) *Amount of required data:* In an application setting, it is desirable to know how many (unlabeled) real frames have

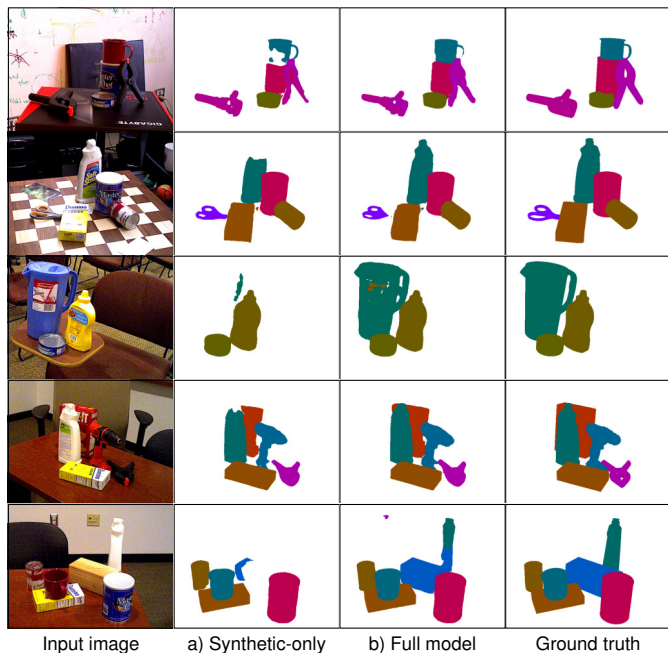


Fig. 6. Qualitative segmentation results on the YCB-Video test set. Compared to a model trained only on synthetic data (a), the predictions of the model trained with SAM regularization (b) are generally more complete.

to be captured. We performed training runs with randomly subsampled training sets on YCB-Video (see Fig. 8). While training with a single real frame hurts performance compared with the purely-synthetic version (compare Table I), gains are observed starting at 10 frames. This shows that our method is very cheap to apply as it does not require extensive dataset capture.

b) *Pseudolabel generation:* Instead of our proposed SAM regularization regime, which can handle overlapping SAM segments, we can also use SAM masks to generate pseudolabels for semantic segmentation. In this case, an exponential moving average (EMA) version of the network under training is used to generate semantic predictions on

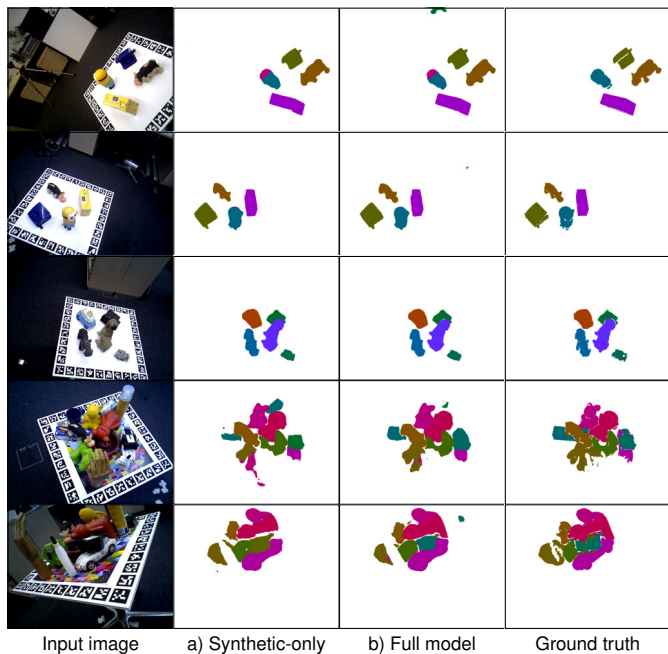


Fig. 7. Qualitative segmentation results on the HomebrewedDB test set. Compared to a model trained only on synthetic data (a), the predictions of the model trained with SAM regularization (b) are more complete and show less classification errors.

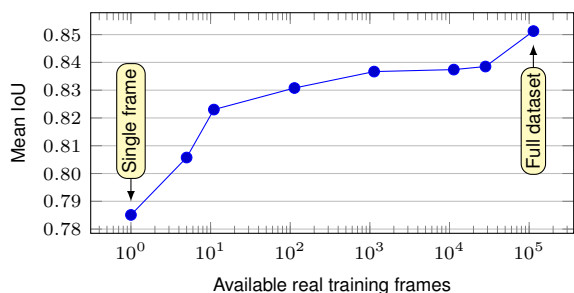


Fig. 8. Sensitivity to amount of real (unlabeled) training data. The model was trained on randomly sampled subsets of the YCB-Video training set. All models were trained for 200 epochs. The full training set has 113k frames.

TABLE II
ADDITIONAL ABLATIONS AND VARIANTS

Experiment	Variant	Mean IoU
Pseudolabels	Synthetic only	0.807
	SAM pseudolabels	0.805
	SAM regularization	0.853
Domain gap	Wider gap (syn only)	0.106
	Wider gap (full)	0.771
Loss scaling	$\alpha = 0.025$	0.832
	$\alpha = 0.05$ (chosen)	0.853
	$\alpha = 0.1$	0.852
Feature dimension	$D = 12$	0.845
	$D = 6$	0.850
	$D = 3$ (chosen)	0.853
Robotic application	Synthetic only	0.704
	Full	0.748

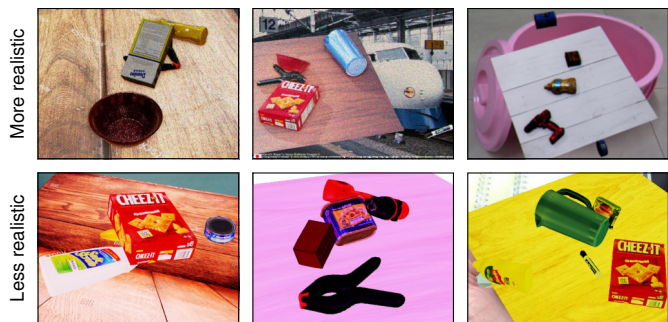


Fig. 9. Widening the domain gap by reducing realism of the synthetic data generator. The bottom row has most available rendering options turned off.

real data. For each object class, a best-fitting SAM mask is found through its IoU with the prediction, thereby generating pseudolabels for further training. Since this training regime cannot be used from scratch due to instability of the generated pseudolabels, we apply it on a model pretrained on synthetic data for 300 epochs. The model is then trained in alternating fashion on synthetic data and the pseudolabeled real data.

In contrast to our SAM regularization, this pseudolabel generation method does not lead to higher generalization ability compared to the baseline trained purely on synthetic data (see Table III). We attribute this to situations where the model under- or oversegments objects in the real domain. In this case, a pseudolabel-based approach is likely to select a SAM mask matching the under-/oversegmentation, not yielding any improvement, whereas our SAM regularization approach will lead the model to consider all possible segmentations found by SAM.

c) Wider domain gap: What if source and target domains are further apart? While domains with completely different styles are not our focus, we can artificially widen the domain gap in a controlled manner by making the synthetic images less realistic. In particular, we switch off the camera noise model, IBL light maps, shadows, and SSAO in the Stillleben generator (see [2] for details). The resulting images are clearly less realistic and less varied (see Fig. 9). Table III shows results from training runs performed with this data, with and without SAM regularization. While the unregularized model clearly overfits on the less-varied source domain data, our proposed SAM regularization restores generalization to real data.

d) The influence of α and D : The loss scaling hyperparameter α was chosen to balance supervision and regularization losses. As one can see in Table III, our model is not very sensitive to this parameter.

While choosing $D = 3$ feature dimensions for the dense feature head is a convenient choice for visualizing features, it is conceivable that higher-dimensional feature spaces might lead to better separation of objects and grouping of parts. However, as Table III shows, an increase to $D = 12$ does not lead to better performance. It is possible to increase D further, but this requires optimization of the variance loss computation due to memory constraints, e.g. by introducing random subsampling.

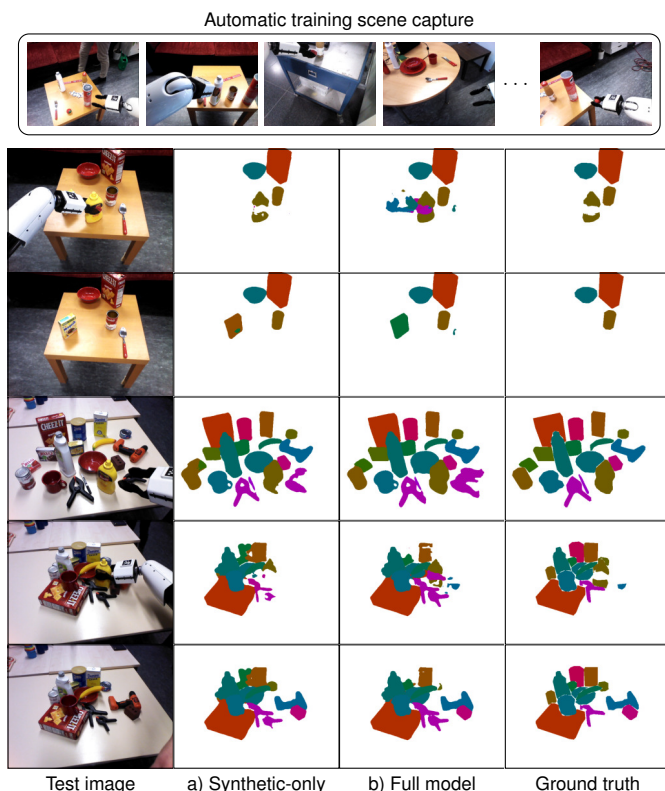


Fig. 10. Qualitative segmentation results on a custom robotic test set. The unlabeled training data was automatically captured during autonomous grasping of operator-specified objects (top). The resulting dataset is used to SAM-regularize a model otherwise trained with labeled synthetic data (a), which gives improved results (b).

F. Application in Robotic Setting

While demonstrating the usefulness of SAM regularization on YCB-Video and HomebrewedDB is interesting, the question remains if it is actually useful in a robotic application. For this purpose, we utilized a PAL Robotics TIAGo++ robot carrying an Orbbec Astra RGB-D camera. Our TIAGo robot is used for research in household contexts and is capable of autonomously grasping user-selected objects. During each such performed grasp, we automatically recorded RGB frames showing the situation before, during, and after the grasp. In this way, we recorded 28 scenes (i.e. object arrangements) with 3-21 frames each, which we divide into 26 train and 2 test scenes.

Both, the quantitative results reported in Table III and the qualitative results shown in Fig. 10, confirm that SAM regularization is also effective in this setting.

V. CONCLUSION

We proposed a practical way to address the annotation bottleneck by using source domain data with annotations and target domain data without annotations, leveraging and learning from a foundation model.

Instead of focusing on improving the quality of the synthetic images, we make use of both domains to achieve a decrease in the Sim2Real gap. Indeed, we have shown that a task-specific regularization using a related foundation model is possible

and beneficial for the task itself. Our method is universally applicable and we demonstrated its advantages for semantic segmentation on two well-known datasets. The evaluation of our method resulted in a mean IoU of 85% and 79% on YCB-Video and HomebrewedDB, a sufficient accuracy for real-world robotic tasks such as grasping.

Furthermore, the regularization term related to the SAM segments results in the learning of meaningful features, which yields the observed improvement in task scores. On YCB-Video, our model trained only on synthetic data and SAM regularization outperformed training on real data. Therefore, we can regularize the model in a task-specific manner so that it performs more robustly in the target domain.

Our method is not restricted to semantic segmentation. Joint training on a task on synthetic data and SAM segment regularization of real data is a generic tool that roboticists can use to reduce the effects of the Sim2Real gap. We are convinced that our method will be applicable to other tasks, such as object detection, panoptic segmentation, 6D pose prediction, and other applications requiring dense features.

REFERENCES

- [1] S. Höfer, K. Bekris, A. Handa, J. C. Gamboa, M. Mozifian, F. Golemo, C. Atkeson, D. Fox, K. Goldberg, J. Leonard, *et al.*, “Sim2Real in robotics and automation: Applications and challenges,” *IEEE Transactions on Automation Science and Engineering*, vol. 18, no. 2, pp. 398–400, 2021.
- [2] M. Schwarz and S. Behnke, “Stilleben: Realistic scene synthesis for deep learning in robotics,” in *IEEE International Conference on Robotics and Automation (ICRA)*, 2020, pp. 10 502–10 508.
- [3] M. Denninger, M. Sundermeyer, D. Winkelbauer, D. Olefir, T. Hodan, Y. Zidan, M. Elbadrawy, M. Knauer, H. Katam, and A. Lodhi, “BlenderProc: Reducing the reality gap with photorealistic rendering,” in *Int. Conference on Robotics: Scienc and Systems (RSS)*, 2020.
- [4] B. T. Imbusch, M. Schwarz, and S. Behnke, “Synthetic-to-real domain adaptation using contrastive unpaired translation,” in *Int. Conference on Automation Science and Engineering (CASE)*, 2022, pp. 595–602.
- [5] A. Kirillov, E. Mintun, N. Ravi, H. Mao, C. Rolland, L. Gustafson, T. Xiao, S. Whitehead, A. C. Berg, W.-Y. Lo, P. Dollár, and R. B. Girshick, “Segment anything,” in *IEEE/CVF International Conference on Computer Vision (ICCV)*, 2023, pp. 3992–4003.
- [6] A. Bardes, J. Ponce, and Y. Lecun, “VICReg: Variance-invariance-covariance regularization for self-supervised learning,” in *International Conference on Learning Representations (ICLR)*, 2022.
- [7] A. Bardes, J. Ponce, and Y. LeCun, “VICRegL: Self-supervised learning of local visual features,” *Advances in Neural Information Processing Systems (NeurIPS)*, vol. 35, pp. 8799–8810, 2022.
- [8] X. Liu, C. Yoo, F. Xing, H. Oh, G. El Fakhri, J.-W. Kang, J. Woo, *et al.*, “Deep unsupervised domain adaptation: A review of recent advances and perspectives,” *APSIPA Transactions on Signal and Information Processing*, vol. 11, no. 1, 2022.
- [9] O. J. Hénaff, S. Koppula, J.-B. Alayrac, A. Van den Oord, O. Vinyals, and J. Carreira, “Efficient visual pretraining with contrastive detection,” in *International Conference on Computer Vision (CVPR)*, 2021.
- [10] T. Park, A. A. Efros, R. Zhang, and J.-Y. Zhu, “Contrastive learning for unpaired image-to-image translation,” in *European Conference on Computer Vision (ECCV)*, Springer, 2020, pp. 319–345.
- [11] J. Devlin, M.-W. Chang, K. Lee, and K. Toutanova, “BERT: Pre-training of deep bidirectional transformers for language understanding,” in *Conference of the North American Chapter of the Association for Computational Linguistics: Human Language Technologies (NAACL-HLT)*, 2019, pp. 4171–4186.
- [12] Y. Liu, M. Ott, N. Goyal, J. Du, M. Joshi, D. Chen, O. Levy, M. Lewis, L. Zettlemoyer, and V. Stoyanov, “RoBERTa: A robustly optimized BERT pretraining approach,” *arXiv preprint arXiv:1907.11692*, 2019.
- [13] OpenAI, “GPT-4 technical report,” *arXiv preprint arXiv:2303.08774*, 2023.

- [14] C. M. Kim, M. Wu, J. Kerr, K. Goldberg, M. Tancik, and A. Kanazawa, "GARField: Group anything with radiance fields," *arXiv preprint arXiv:2401.09419*, 2024.
- [15] T. Xiao, Y. Liu, B. Zhou, Y. Jiang, and J. Sun, "Unified perceptual parsing for scene understanding," in *European Conference on Computer Vision (ECCV)*, 2018, pp. 418–434.
- [16] A. Kirillov, R. Girshick, K. He, and P. Dollár, "Panoptic feature pyramid networks," in *Conference on Computer Vision and Pattern Recognition (CVPR)*, 2019, pp. 6399–6408.
- [17] Z. Liu, H. Mao, C.-Y. Wu, C. Feichtenhofer, T. Darrell, and S. Xie, "A ConvNet for the 2020s," in *Conference on Computer Vision and Pattern Recognition (CVPR)*, 2022, pp. 11 976–11 986.
- [18] T.-Y. Lin, P. Dollár, R. Girshick, K. He, B. Hariharan, and S. Belongie, "Feature pyramid networks for object detection," in *Conference on computer vision and pattern recognition (CVPR)*, 2017.
- [19] H. Zhao, J. Shi, X. Qi, X. Wang, and J. Jia, "Pyramid scene parsing network," in *Conference on Computer Vision and Pattern Recognition (CVPR)*, 2017, pp. 2881–2890.
- [20] P. R. Florence, L. Manuelli, and R. Tedrake, "Dense object nets: Learning dense visual object descriptors by and for robotic manipulation," in *Conference on Robot Learning (CoRL)*, PMLR, 2018, pp. 373–385.
- [21] Y. Xiang, T. Schmidt, V. Narayanan, and D. Fox, "PoseCNN: A convolutional neural network for 6D object pose estimation in cluttered scenes," *Robotics: Science and Systems (RSS)*, 2018.
- [22] R. Kaskman, S. Zakharov, I. Shugurov, and S. Ilic, "HomebrewedDB: RGB-D dataset for 6D pose estimation of 3D objects," in *International Conference on Computer Vision Workshops (CVPR)*, 2019.
- [23] M. Sundermeyer, T. Hodaň, Y. Labbe, G. Wang, E. Brachmann, B. Drost, C. Rother, and J. Matas, "BOP challenge 2022 on detection, segmentation and pose estimation of specific rigid objects," in *Conference on Computer Vision and Pattern Recognition (CVPR)*, 2023.
- [24] B. Calli, A. Singh, A. Walsman, S. Srinivasa, P. Abbeel, and A. M. Dollar, "The YCB object and model set: Towards common benchmarks for manipulation research," in *International Conference on Advanced Robotics (ICAR)*, 2015, pp. 510–517.
- [25] G. Lin, A. Milan, C. Shen, and I. Reid, "RefineNet: Multi-path refinement networks for high-resolution semantic segmentation," in *Conference on Computer Vision and Pattern Recognition (CVPR)*, 2017, pp. 1925–1934.

APPENDIX

A. Additional Ablations

We present additional ablations in Table III which investigate further hyperparameters and evaluate these on the YCB-Video dataset.

We first introduce an additional balancing factor β for the loss introduced in Equation 6:

$$\mathcal{L}_{\text{real}} = \alpha (\beta \mathcal{L}_{\text{Inv}} + (2 - \beta) \mathcal{L}_{\text{Var}}) \quad (9)$$

Note that $\beta = 1$ represents the original version with equal balancing. As can be seen in Table III, a minor performance increase can be gained by decreasing the importance of the invariance loss ($\beta = 0.5$), yielding to stronger separation of segments in feature space.

We also investigate *smaller* values for D in Table III. Even for $D = 1$ the model manages to properly separate segments in the resulting one-dimensional feature space (see Fig. 11) and the SAM regularization scheme remains effective.

TABLE III
SUPPLEMENTARY ABLATIONS ON YCB-VIDEO

Experiment	Variant	Mean IoU
Invariance/Variance balance	$\beta = 1$	0.853
	$\beta = 0.5$	0.857
	$\beta = 1.5$	0.850
Feature dimension	$D = 12$	0.845
	$D = 6$	0.850
	$D = 3$ (chosen)	0.853
	$D = 2$	0.847
	$D = 1$	0.847

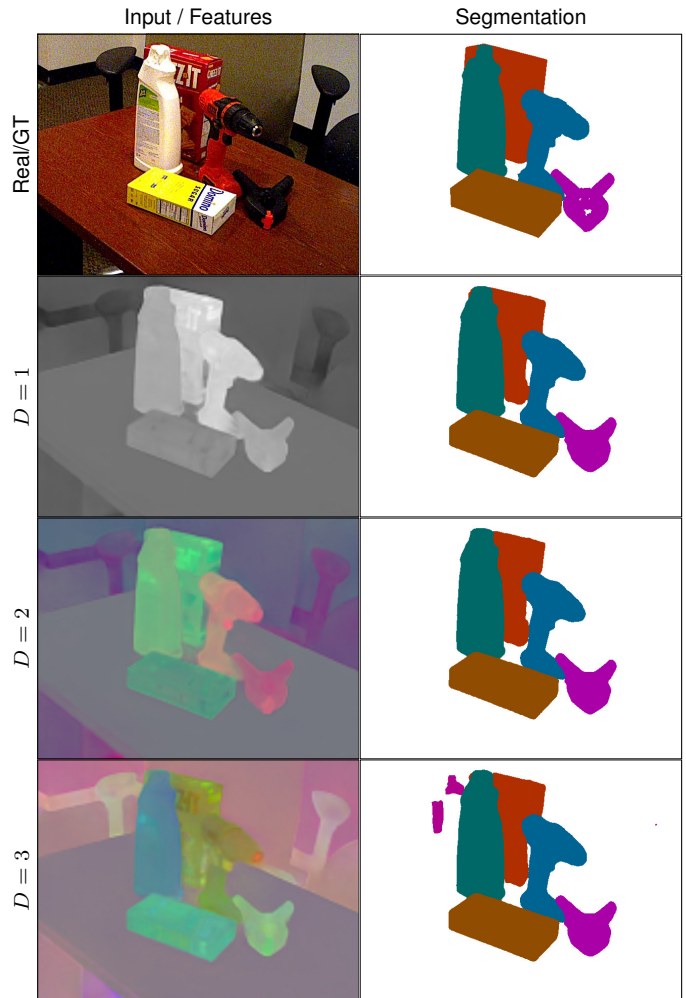


Fig. 11. Qualitative examples of dense features learned with different D values. To visualize $D = 2$, the blue channel is set to a constant value. $D = 1$ is visualized as grayscale.